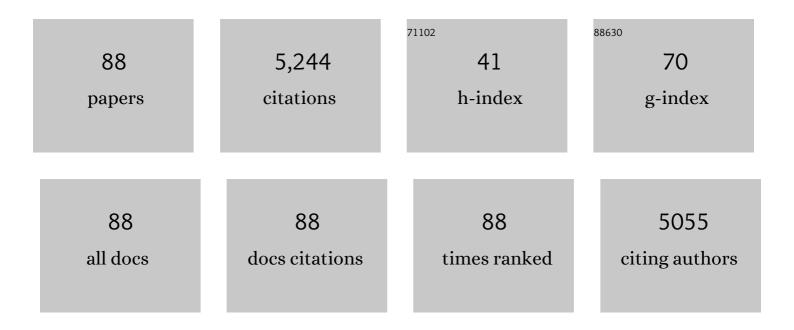
List of Publications by Year in descending order

Source: https://exaly.com/author-pdf/2820171/publications.pdf Version: 2024-02-01



WENIUN DONG

#	Article	IF	CITATIONS
1	Shape-stabilized phase change materials based on porous supports for thermal energy storage applications. Chemical Engineering Journal, 2019, 356, 641-661.	12.7	459
2	Nanoconfinement effects on thermal properties of nanoporous shape-stabilized composite PCMs: A review. Nano Energy, 2018, 53, 769-797.	16.0	260
3	Highly graphitized 3D network carbon for shape-stabilized composite PCMs with superior thermal energy harvesting. Nano Energy, 2018, 49, 86-94.	16.0	200
4	Optimization strategies of composite phase change materials for thermal energy storage, transfer, conversion and utilization. Energy and Environmental Science, 2020, 13, 4498-4535.	30.8	181
5	Surface functionalization engineering driven crystallization behavior of polyethylene glycol confined in mesoporous silica for shape-stabilized phase change materials. Nano Energy, 2016, 19, 78-87.	16.0	172
6	A sandwich-like heterostructure of TiO 2 nanosheets with MIL-100(Fe): A platform for efficient visible-light-driven photocatalysis. Applied Catalysis B: Environmental, 2017, 209, 506-513.	20.2	149
7	Boosting Photocatalytic Hydrogen Production via Interfacial Engineering on 2D Ultrathin Zâ€6cheme ZnIn ₂ S ₄ /g ₃ N ₄ Heterojunction. Advanced Functional Materials, 2022, 32, .	14.9	147
8	Hydrothermal synthesis and structure evolution of hierarchical cobalt sulfidenanostructures. Dalton Transactions, 2011, 40, 243-248.	3.3	146
9	Introduction of organic-organic eutectic PCM in mesoporous N-doped carbons for enhanced thermal conductivity and energy storage capacity. Applied Energy, 2018, 211, 1203-1215.	10.1	137
10	Carbon nanotube bundles assembled flexible hierarchical framework based phase change material composites for thermal energy harvesting and thermotherapy. Energy Storage Materials, 2020, 26, 129-137.	18.0	124
11	Bidentate carboxylate linked TiO2 with NH2-MIL-101(Fe) photocatalyst: a conjugation effect platform for high photocatalytic activity under visible light irradiation. Science Bulletin, 2020, 65, 658-669.	9.0	117
12	Synthesis of porous carbon from cotton using an Mg(OH) ₂ template for form-stabilized phase change materials with high encapsulation capacity, transition enthalpy and reliability. Journal of Materials Chemistry A, 2018, 6, 8969-8977.	10.3	106
13	Smart integration of carbon quantum dots in metal-organic frameworks for fluorescence-functionalized phase change materials. Energy Storage Materials, 2019, 18, 349-355.	18.0	105
14	Multifunctional Nanowire Bioscaffolds on Titanium. Chemistry of Materials, 2007, 19, 4454-4459.	6.7	102
15	A novel enhancement of shape/thermal stability and energy-storage capacity of phase change materials through the formation of composites with 3D porous (3,6)-connected metal–organic framework. Chemical Engineering Journal, 2020, 389, 124430.	12.7	99
16	General Approach to Well-Defined Perovskite MTiO ₃ (M = Ba, Sr, Ca, and Mg) Nanostructures. Journal of Physical Chemistry C, 2011, 115, 3918-3925.	3.1	96
17	Core-sheath structural carbon materials for integrated enhancement of thermal conductivity and capacity. Applied Energy, 2018, 217, 369-376.	10.1	91
18	Hierarchically nanostructured MnCo ₂ O ₄ as active catalysts for the synthesis of N-benzylideneaniline from benzyl alcohol and aniline. Green Chemistry, 2017, 19, 769-777.	9.0	89

#	Article	IF	CITATIONS
19	Light-facilitated structure reconstruction on self-optimized photocatalyst TiO2@BiOCl for selectively efficient conversion of CO2 to CH4. Applied Catalysis B: Environmental, 2021, 286, 119832.	20.2	87
20	Nanoconfinement effects of N-doped hierarchical carbon on thermal behaviors of organic phase change materials. Energy Storage Materials, 2019, 18, 280-288.	18.0	86
21	Hierarchical 3D Reduced Graphene Porous-Carbon-Based PCMs for Superior Thermal Energy Storage Performance. ACS Applied Materials & Interfaces, 2018, 10, 32093-32101.	8.0	85
22	The structural and biological properties of hydroxyapatite-modified titanate nanowire scaffolds. Biomaterials, 2011, 32, 5837-5846.	11.4	82
23	A sustainable method toward melamine-based conjugated polymer semiconductors for efficient photocatalytic hydrogen production under visible light. Green Chemistry, 2018, 20, 664-670.	9.0	77
24	Highly porous carbons derived from MOFs for shape-stabilized phase change materials with high storage capacity and thermal conductivity. RSC Advances, 2016, 6, 40106-40114.	3.6	71
25	Multifunctional, Catalytic Nanowire Membranes and the Membrane-Based 3D Devices. Journal of Physical Chemistry B, 2006, 110, 16819-16822.	2.6	70
26	Photocatalytic Degradation of Acid Chrome Blue K with Porphyrin-Sensitized TiO ₂ under Visible Light. Journal of Physical Chemistry C, 2008, 112, 14878-14882.	3.1	67
27	Heterogeneous Fe-MIL-101 catalysts for efficient one-pot four-component coupling synthesis of highly substituted pyrroles. New Journal of Chemistry, 2015, 39, 4919-4923.	2.8	67
28	Co(<scp>ii</scp>) complexes loaded into metal–organic frameworks as efficient heterogeneous catalysts for aerobic epoxidation of olefins. Catalysis Science and Technology, 2016, 6, 161-168.	4.1	66
29	Boosting photocatalytic hydrogen evolution: Orbital redistribution of ultrathin ZnIn2S4 nanosheets via atomic defects. Applied Catalysis B: Environmental, 2022, 305, 121007.	20.2	61
30	Construction of TiO2 nanosheets/tetra (4-carboxyphenyl) porphyrin hybrids for efficient visible-light photoreduction of CO2. Chemical Engineering Journal, 2019, 374, 684-693.	12.7	56
31	Ni, In co-doped ZnIn2S4 for efficient hydrogen evolution: Modulating charge flow and balancing H adsorption/desorption. Applied Catalysis B: Environmental, 2022, 310, 121337.	20.2	55
32	A performance study of enhanced visible-light-driven photocatalysis and magnetical protein separation of multifunctional yolk–shell nanostructures. Journal of Materials Chemistry A, 2013, 1, 10030.	10.3	54
33	Construction of covalently integrated core-shell TiO2 nanobelts@COF hybrids for highly selective oxidation of alcohols under visible light. Applied Surface Science, 2019, 493, 551-560.	6.1	53
34	Oneâ€Pot Preparation of Hierarchical Nanosheetâ€Constructed Fe ₃ O ₄ /MILâ€88B(Fe) Magnetic Microspheres with High Efficiency Photocatalytic Degradation of Dye. ChemCatChem, 2016, 8, 3510-3517.	3.7	52
35	A facile one-step synthesis of porous N-doped carbon from MOF for efficient thermal energy storage capacity of shape-stabilized phase change materials. Materials Today Energy, 2019, 12, 239-249.	4.7	51
36	Synthesis and Characterization of Paraffin/Metal Organic Gel Derived Porous Carbon/Boron Nitride Composite Phase Change Materials for Thermal Energy Storage. European Journal of Inorganic Chemistry, 2018, 2018, 5167-5175.	2.0	47

#	Article	IF	CITATIONS
37	Alkylated Mesoâ€Macroporous Metal–Organic Framework Hollow Tubes as Nanocontainers of Octadecane for Energy Storage and Thermal Regulation. Small, 2018, 14, e1801970.	10.0	46
38	Synthesis of Heparin-Immobilized, Magnetically Addressable Cellulose Nanofibers for Biomedical Applications. ACS Biomaterials Science and Engineering, 2016, 2, 1905-1913.	5.2	44
39	Ambient pressure dried flexible silica aerogel for construction of monolithic shape-stabilized phase change materials. Solar Energy Materials and Solar Cells, 2019, 201, 110122.	6.2	44
40	Highly dispersed Pt clusters encapsulated in MIL-125-NH2 via in situ auto-reduction method for photocatalytic H2 production under visible light. Nano Research, 2021, 14, 4250-4257.	10.4	43
41	Synthesis of a Fe ₃ O ₄ –CuO@meso-SiO ₂ nanostructure as a magnetically recyclable and efficient catalyst for styrene epoxidation. Catalysis Science and Technology, 2014, 4, 3082-3089.	4.1	41
42	Highly efficient sulfonated-polystyrene–Cu(II)@Cu ₃ (BTC) ₂ core–shell microsphere catalysts for base-free aerobic oxidation of alcohols. Journal of Materials Chemistry A, 2015, 3, 4266-4273.	10.3	41
43	Vacuum-Dried Synthesis of Low-Density Hydrophobic Monolithic Bridged Silsesquioxane Aerogels for Oil/Water Separation: Effects of Acid Catalyst and Its Excellent Flexibility. ACS Applied Nano Materials, 2018, 1, 933-939.	5.0	39
44	Phase change materials stabilized by porous metal supramolecular gels: Gelation effect on loading capacity and thermal performance. Chemical Engineering Journal, 2020, 394, 124806.	12.7	39
45	Shapeâ€Stabilized Phase Change Materials Based on Stearic Acid and Mesoporous Hollow SiO ₂ Microspheres (SA/SiO ₂) for Thermal Energy Storage. European Journal of Inorganic Chemistry, 2017, 2017, 2138-2143.	2.0	37
46	SO ₃ H-functionalized metal organic frameworks: an efficient heterogeneous catalyst for the synthesis of quinoxaline and derivatives. RSC Advances, 2016, 6, 35135-35143.	3.6	35
47	Preparation of hollow Ag/Pt heterostructures on TiO2 nanowires and their catalytic properties. Applied Catalysis B: Environmental, 2016, 180, 344-350.	20.2	35
48	Synthesis of highly loaded and well dispersed CuO/SBA-15 via an ultrasonic post-grafting method and its application as a catalyst for the direct hydroxylation of benzene to phenol. Microporous and Mesoporous Materials, 2013, 177, 47-53.	4.4	34
49	Carbon inserted defect-rich MoS2â^'X nanosheets@CdSnanospheres for efficient photocatalytic hydrogen evolution under visible light irradiation. Journal of Colloid and Interface Science, 2020, 569, 89-100.	9.4	34
50	Functionalization of electrospun nanofibers of natural cotton cellulose by cerium dioxide nanoparticles for ultraviolet protection. Journal of Applied Polymer Science, 2013, 130, 1524-1529.	2.6	33
51	Preparation of hollow multiple-Ag-nanoclustes-C-shell nanostructures and their catalytic properties. Applied Catalysis B: Environmental, 2016, 180, 13-19.	20.2	31
52	3D Self-Supported Porous NiO@NiMoO ₄ Core–Shell Nanosheets for Highly Efficient Oxygen Evolution Reaction. Inorganic Chemistry, 2019, 58, 6758-6764.	4.0	31
53	Biodegradable and Bioactive PCL–PGS Core–Shell Fibers for Tissue Engineering. ACS Omega, 2017, 2, 6321-6328.	3.5	30
54	Controlled Synthesis of 3D Flowerâ€like Ni ₂ P Composed of Mesoporous Nanoplates for Overall Water Splitting. Chemistry - an Asian Journal, 2017, 12, 2956-2961.	3.3	30

#	Article	IF	CITATIONS
55	One-pot synthesis of Ag@SiO ₂ @Ag sandwich nanostructures. Nanotechnology, 2010, 21, 245602.	2.6	29
56	Hierarchical α-Ni(OH) ₂ Composed of Ultrathin Nanosheets with Controlled Interlayer Distances and Their Enhanced Catalytic Performance. ACS Applied Materials & Interfaces, 2017, 9, 20476-20483.	8.0	29
57	One-pot synthesis of light-driven polymeric composite phase change materials based on N-doped porous carbon for enhanced latent heat storage capacity and thermal conductivity. Solar Energy Materials and Solar Cells, 2018, 179, 392-400.	6.2	29
58	Controllable synthesis and surface modification of molybdenum oxide nanowires: a short review. Tungsten, 2019, 1, 258-265.	4.8	28
59	In-situ derived graphene from solid sodium acetate for enhanced photothermal conversion, thermal conductivity, and energy storage capacity of phase change materials. Solar Energy Materials and Solar Cells, 2020, 205, 110269.	6.2	28
60	Network Structural CNTs Penetrate Porous Carbon Support for Phaseâ€Change Materials with Enhanced Electroâ€Thermal Performance. Advanced Electronic Materials, 2020, 6, 1901428.	5.1	26
61	Bionic sunflower-like structure of polydopamine-confined NiFe-based quantum dots for electrocatalytic oxygen evolution reaction. Applied Catalysis B: Environmental, 2022, 302, 120833.	20.2	25
62	Fabrication and characterization of electrospun nanofibers of high DP natural cotton lines cellulose. Fibers and Polymers, 2011, 12, 345-351.	2.1	24
63	PEG encapsulated by porous triamide-linked polymers as support for solid-liquid phase change materials for energy storage. Chemical Physics Letters, 2017, 671, 165-173.	2.6	24
64	Cu@Cu ₃ P Core–Shell Nanowires Attached to Nickel Foam as Highâ€Performance Electrocatalysts for the Hydrogen Evolution Reaction. Chemistry - A European Journal, 2019, 25, 1083-1089.	3.3	24
65	One-Pot Redox Syntheses of Heteronanostructures of Ag Nanoparticles on MoO3Nanofibers. Journal of Physical Chemistry B, 2006, 110, 5845-5848.	2.6	23
66	Room-temperature solution synthesis of Ag nanoparticle functionalized molybdenum oxide nanowires and their catalytic applications. Nanotechnology, 2012, 23, 425602.	2.6	23
67	Imine-linked micron-network polymers with high polyethylene glycol uptake for shaped-stabilized phase change materials. RSC Advances, 2016, 6, 44807-44813.	3.6	23
68	A one-step in-situ assembly strategy to construct PEG@MOG-100-Fe shape-stabilized composite phase change material with enhanced storage capacity for thermal energy storage. Chemical Physics Letters, 2018, 695, 99-106.	2.6	23
69	Controlled synthesis and self-assembly of dendrite patterns of Fe ₃ O ₄ nanoparticles. Nanotechnology, 2009, 20, 035601.	2.6	22
70	Porous organic–inorganic hybrid xerogels for stearic acid shape-stabilized phase change materials. New Journal of Chemistry, 2017, 41, 1790-1797.	2.8	22
71	Difference between Metal-S and Metal-O Bond Orders: A Descriptor of Oxygen Evolution Activity for Isolated Metal Atom-Doped MoS2 Nanosheets. IScience, 2019, 20, 481-488.	4.1	21
72	Atomically dispersed ruthenium sites on whisker-like secondary microstructure of porous carbon host toward highly efficient hydrogen evolution. Journal of Materials Chemistry A, 2020, 8, 3203-3210.	10.3	20

#	Article	IF	CITATIONS
73	Self-assembly engineering toward large-area defect-rich TiO2(B) nanosheets-based free-standing films for high-performance lithium-ion batteries. Journal of Power Sources, 2020, 448, 227458.	7.8	18
74	Construction of dual-Z-scheme WS2-WO3·H2O/g-C3N4 catalyst for photocatalytic H2 evolution under visible light. Chemical Engineering Journal, 2021, 426, 130822.	12.7	18
75	The reinforced photothermal effect of conjugated dye/graphene oxide-based phase change materials: Fluorescence resonance energy transfer and applications in solar-thermal energy storage. Chemical Engineering Journal, 2022, 428, 130605.	12.7	17
76	The formation and UV-blocking property of flower-like ZnO nanorod on electrospun natural cotton cellulose nanofibers. Fibers and Polymers, 2014, 15, 281-285.	2.1	16
77	Hierarchical nitrogen-doped porous carbon incorporating cobalt nanocrystal sites for nitrophenol reduction. Chemical Engineering Science, 2020, 217, 115525.	3.8	16
78	Approaching Theoretical Capacities in Thick Lithium Vanadium Phosphate Electrodes at High Charge/Discharge Rates. ACS Sustainable Chemistry and Engineering, 2018, 6, 15608-15617.	6.7	14
79	Inâ€situ Selfâ€transformation Synthesis of Nâ€doped Carbon Coating Paragenetic Anatase/Rutile Heterostructure with Enhanced Photocatalytic CO ₂ Reduction Activity. ChemCatChem, 2020, 12, 3274-3284.	3.7	14
80	Hetero-nanostructure of silver nanoparticles on MO x (M = Mo, Ti and Si) and their applications. Science China Chemistry, 2011, 54, 865.	8.2	11
81	A Facile Approach for Transferring PbS Colloidal Photonic Structures into Alkanol Solutions and Composite Solid Films. European Journal of Inorganic Chemistry, 2012, 2012, 1204-1209.	2.0	8
82	Microstructural evolution and mechanical properties of hot pressed WC–α-Al ₂ O ₃ with Y ₂ O ₃ and CeO ₂ . Advances in Applied Ceramics, 2016, 115, 316-321.	1.1	8
83	Synthesis of N-TiO2@NH2-MIL-88(Fe) Core-shell Structure for Efficient Fenton Effect Assisted Methylene Blue Degradation Under Visible Light. Chemical Research in Chinese Universities, 2020, 36, 1068-1075.	2.6	8
84	Fabrication and Elastic Properties of TiO ₂ Nanohelix Arrays through a Pressure-Induced Hydrothermal Method. ACS Nano, 2021, 15, 14174-14184.	14.6	7
85	Formation of the First Derivatives of Endohedral Diterbium Fullerenes via Carbene Addition to a Large Carbon Cage. Fullerenes Nanotubes and Carbon Nanostructures, 2015, 23, 1018-1023.	2.1	4
86	Assembly of flexible nanohelix films: stress–exporting insights into the electrochemical performance of lithium–ion batteries. Materials Today Nano, 2021, 16, 100141.	4.6	4
87	Highlights on inorganic solid state chemistry and energy materials. Science China Technological Sciences, 2012, 55, 3248-3252.	4.0	2
88	A simple approach to porous low-temperature-sintering BaTiO3. Science China Chemistry, 2012, 55, 1765-1769.	8.2	2